AMERICAN SOCIETY FOR MICROBIOLOGY | mBio®

RESEARCH ARTICLE
Molecular Biology and Physiology

A Novel Role of Fungal Type I Myosin in Regulating Membrane Properties and Its Association with D-Amino Acid Utilization in *Cryptococcus gattii*

Ami Khanal Lamichhane,[a] H. Martin Garraffo,[b] Hongyi Cai,[b] Peter J. Walter,[b] Kyung J. Kwon-Chung,[a] Yun C. Chang[a]

[a]Molecular Microbiology Section, Laboratory of Clinical Immunology and Microbiology, NIAID, NIH, Bethesda, Maryland, USA
[b]Clinical Mass Spectrometry Core, NIDDK, NIH, Bethesda, Maryland, USA

ABSTRACT We found a novel role of Myo5, a type I myosin (myosin-I), and its fortuitous association with D-amino acid utilization in *Cryptococcus gattii*. Myo5 colocalized with actin cortical patches and was required for endocytosis. Interestingly, the *myo5*Δ mutant accumulated high levels of D-proline and D-alanine which caused toxicity in *C. gattii* cells. The *myo5*Δ mutant also accumulated a large set of substrates, such as membrane-permeant as well as non-membrane-permeant dyes, L-proline, L-alanine, and flucytosine intracellularly. Furthermore, the efflux rate of fluorescein was significantly increased in the *myo5*Δ mutant. Importantly, the endocytic defect of the *myo5*Δ mutant did not affect the localization of the proline permease and flucytosine transporter. These data indicate that the substrate accumulation phenotype is not solely due to a defect in endocytosis, but the membrane properties may have been altered in the *myo5*Δ mutant. Consistent with this, the sterol staining pattern of the *myo5*Δ mutant was different from that of the wild type, and the mutant was hypersensitive to amphotericin B. It appears that the changes in sterol distribution may have caused altered membrane permeability in the *myo5*Δ mutant, allowing increased accumulation of substrate. Moreover, myosin-I mutants generated in several other yeast species displayed a similar substrate accumulation phenotype. Thus, fungal type I myosin appears to play an important role in regulating membrane permeability. Although the substrate accumulation phenotype was detected in strains with mutations in the genes involved in actin nucleation, the phenotype was not shared in all endocytic mutants, indicating a complicated relationship between substrate accumulation and endocytosis.

IMPORTANCE *Cryptococcus gattii*, one of the etiological agents of cryptococcosis, can be distinguished from its sister species *Cryptococcus neoformans* by growth on D-amino acids. *C. gattii MYO5* affected the growth of *C. gattii* on D-amino acids. The *myo5*Δ cells accumulated high levels of various substrates from outside the cells, and excessively accumulated D-amino acids appeared to have caused toxicity in the *myo5*Δ cells. We provide evidence on the alteration of membrane properties in the *myo5*Δ mutants. Additionally, alteration in the *myo5*Δ membrane permeability causing higher substrate accumulation is associated with the changes in the sterol distribution. Furthermore, myosin-I in three other yeasts also manifested a similar role in substrate accumulation. Thus, while fungal myosin-I may function as a classical myosin-I, it has hitherto unknown additional roles in regulating membrane permeability. Since deletion of fungal myosin-I causes significantly elevated susceptibility to multiple antifungal drugs, it could serve as an effective target for augmentation of fungal therapy.

KEYWORDS *Cryptococcus*, actin patches, endocytosis, membrane permeability, myosin-I

Citation Khanal Lamichhane A, Garraffo HM, Cai H, Walter PJ, Kwon-Chung KJ, Chang YC. 2019. A novel role of fungal type I myosin in regulating membrane properties and its association with D-amino acid utilization in *Cryptococcus gattii*. mBio 10:e01867-19. https://doi.org/10.1128/mBio.01867-19.

Editor James W. Kronstad, University of British Columbia

Address correspondence to Yun C. Chang, ychang@niaid.nih.gov.

This article is a direct contribution from a Fellow of the American Academy of Microbiology. Solicited external reviewers: J. Andrew Alspaugh, Duke University Medical Center; Scott Filler, Los Angeles Biomedical Research Institute at Harbor-UCLA Medical Center.

Received 15 July 2019
Accepted 2 August 2019
Published 27 August 2019

Type I myosin (myosin-I) belongs to a large superfamily of actin-dependent molecular motors (1) and plays important roles in diverse cellular processes such as polarized morphogenesis, cell migration, and endocytosis (for reviews, see references 2 to 7). Myosin-I is composed of a globular head or motor domain and neck and tail of various lengths. The head or motor domain binds to actin in an ATP-dependent manner and generates force by ATP hydrolysis. The N-terminal head region is connected to the neck which consists of an IQ motif that provides binding sites for myosin light chains. The carboxyl-terminal tail contains TH1 and TH2 (tail homology 1 and 2) and SH3 domains which are thought to specify the role of myosin-I in protein-protein interactions, membrane binding, and intracellular signaling. Myosin-I has been extensively studied in several yeast species. For instance, *MYO3* and *MYO5* are the two myosin-I-encoding genes in *Saccharomyces cerevisiae*, and both Myo5 and Myo3 are colocalized with actin cortical patches (8). Deletion of either *MYO3* or *MYO5* is tolerated by cells, but a deletion of both genes causes defects in endocytosis as well as in growth (9, 10). Myo5 of *Candida albicans* is also colocalized with actin patches at the bud and hyphal tips, and the *myo5* mutant is impaired in polarized growth, hyphal formation, and endocytosis (11, 12). Also, disruption of *myo1* in *Schizosaccharomyces pombe* causes growth retardation and aberrance in cell morphology associated with an abnormal distribution of F-actin patches (13, 14).

Cryptococcus gattii and *Cryptococcus neoformans* are two closely related basidiomycetous yeasts that cause cryptococcosis in humans and animals (15). The ability to utilize D-proline or D-alanine as the sole source of nitrogen can be used to differentiate *C. gattii* isolates from *C. neoformans* isolates (16, 17). D-Amino acids have been found in the mammalian forebrain and various tissues (18–20). In addition, plants synthesize D-amino acid derivatives, and some D-amino acids, such as D-alanine, are widely found in higher plants (21, 22). Since the major ecological niche of *C. gattii* is plants (15), D-amino acid utilization may bear significance in pathobiology as well as ecology of the species. During the screening of a library constructed by T-DNA insertion in *C. gattii* strain R-265, we isolated a clone that failed to grow robustly on D-proline as the sole nitrogen source (23). The clone was identified to have an insertion in the gene encoding the putative type I myosin (CNBG_4524). Although myosin-I is involved in diverse cellular processes, there is no report of myosin-I function related to D-amino acid utilization. This observation prompted us to explore the function of the *C. gattii* myosin-I gene, which we designated *MYO5*. Myo5 was found to colocalize with actin cortical patches and was required for endocytosis. We further established the possible cause of how the *myo5* mutant failed to grow when D-proline was the sole source of nitrogen. Unexpectedly, deletion of *MYO5* caused higher accumulation of D-proline, which is toxic and thereby restricted the growth of the *myo5*Δ mutant on D-proline. We hypothesize and provide evidence that the properties of the cell membrane in the *myo5* mutant have been altered to cause higher accumulation of foreign substrates inside the cells. Furthermore, we demonstrated that similar phenotypes are also conserved in *C. neoformans* and two other well-studied yeast species unrelated to *Cryptococcus*.

RESULTS

***MYO5* deletion in *C. gattii* causes growth defects on D-amino acids.** To further characterize the role of *MYO5* in the utilization of D-amino acids, we deleted the *MYO5* gene in the *C. gattii* strain R265. The *myo5*Δ mutant was viable, and its growth was only slightly reduced on YEPD and YNB media (Fig. 1A). The *myo5*Δ mutant, however, grew poorly on media containing D-proline, and growth was also clearly reduced on media with D-alanine as the sole nitrogen source (Fig. 1A). Reconstitution of the *myo5*Δ mutant with the wild-type *MYO5* complemented the growth defects on these media, indicating that *MYO5* plays a hitherto unidentified role in D-amino acid utilization.

Myo5 functions as classical type I myosin. It has been shown that myosin-I is located at cortical actin patches in several fungi (8, 12). To determine whether Myo5 is associated with actin, we tagged Myo5 with green fluorescent protein, mNG (24), at its

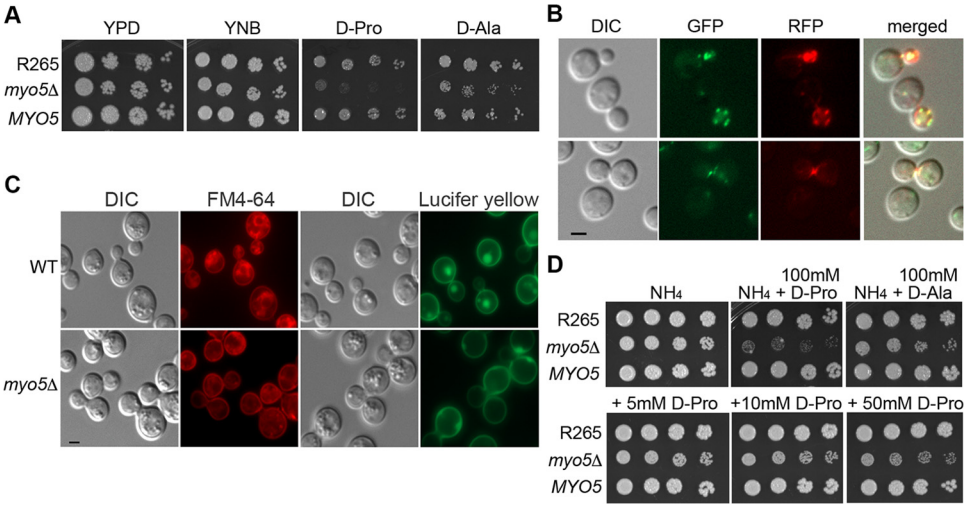

FIG 1 Identification of *MYO5* function. (A) *MYO5* is important for D-proline utilization. Cells of the wild type, the *myo5*Δ mutant, and the *myo5*Δ complemented strain (*MYO5*) were serially diluted and spotted on the indicated media. Plates were incubated at 30°C for 3 days and photographed. (B) Myo5 is colocalized with actin cortical patches. Myo5 was tagged with green fluorescent protein (GFP) (green color). Actin was visualized with Lifeact-RFP (red color). Fluorescent and differential interference contrast (DIC) images were taken from log-phase cells. (C) *MYO5* is involved in endocytosis. Cells were stained with FM4-64 to determine membrane internalization (DIC and FM4-64 columns) or stained with Lucifer yellow to determine fluid phase endocytosis (DIC and Lucifer yellow columns). For FM4-64 staining, cells were stained with 16 μM FM4-64 on ice for 15 min, washed, and incubated in YEPD for 80 min before imaging. Bar = 2 μm. WT, wild type. (D) D-Amino acids are toxic to the *myo5*Δ mutant. Cells were serially diluted and spotted on media containing 10 mM ammonium sulfate (NH_4) with or without supplementation with 100 mM D-proline or D-alanine (top row). Cells were also spotted on NH_4 media supplemented with 5, 10, or 50 mM D-proline (bottom row). Plates were incubated at 30°C for 3 days and photographed.

C terminus. Homologous integration of Myo5-mNG into the *myo5*Δ locus complemented the *myo5*Δ mutant's growth defect in D-proline, suggesting that tagging of Myo5 with mNG did not interfere with its function. To determine whether Myo5 is localized to cortical actin patches, we transformed the Lifeact-RFP plasmid to the Myo5-mNG-tagged strain. Lifeact has a 17-amino-acid peptide sequence of Abp140 from *S. cerevisiae* which is a versatile marker for localization of actin (25), and Lifeact-RFP has stained typical actin patches and cables in *C. neoformans* (26). We found that Myo5-mNG colocalized with Lifeact-RFP at cortical actin patches (Fig. 1B, top row) and occasionally at the isthmus between the mother and daughter cells (Fig. 1B, bottom row).

To determine whether the cryptococcal Myo5 functions as a classical myosin-I, we investigated the effect of *MYO5* deletion on endocytosis. First, FM4-64, a styryl dye, was used to determine the behavior of membrane internalization. When the R265 cells were stained with FM4-64, bright ring-like structures inside cells depicting the endosomes were observed (Fig. 1C, DIC and FM4-64 columns). However, *myo5*Δ cells stained with FM4-64 lacked bright ring-like structure inside the cell, and most of the FM4-64 staining was on the cell membrane. Second, analysis of fluid phase endocytosis with Lucifer yellow revealed that the dye was internalized and trafficked to vacuoles in the wild type but not in the *myo5*Δ mutant (Fig. 1C, DIC and Lucifer yellow columns). These results suggested that the *myo5*Δ mutant was defective in endocytosis. Thus, cryptococcal Myo5 behaves as a classical myosin-I in relation to endocytosis, as is the case in several other fungi.

***MYO5* is involved in substrate accumulation.** We showed that *C. gattii* Myo5 behaves as a typical type I myosin. However, the involvement of myosin-I in the utilization of D-amino acids as the sole nitrogen source remained obscure. D-Amino acids have been reported to be toxic to animals and plants (27–29). Although the growth of the wild type was not affected on defined media containing 10 mM ammonium sulfate supplemented with 100 mM D-proline or 100 mM L-proline, the *myo5*Δ

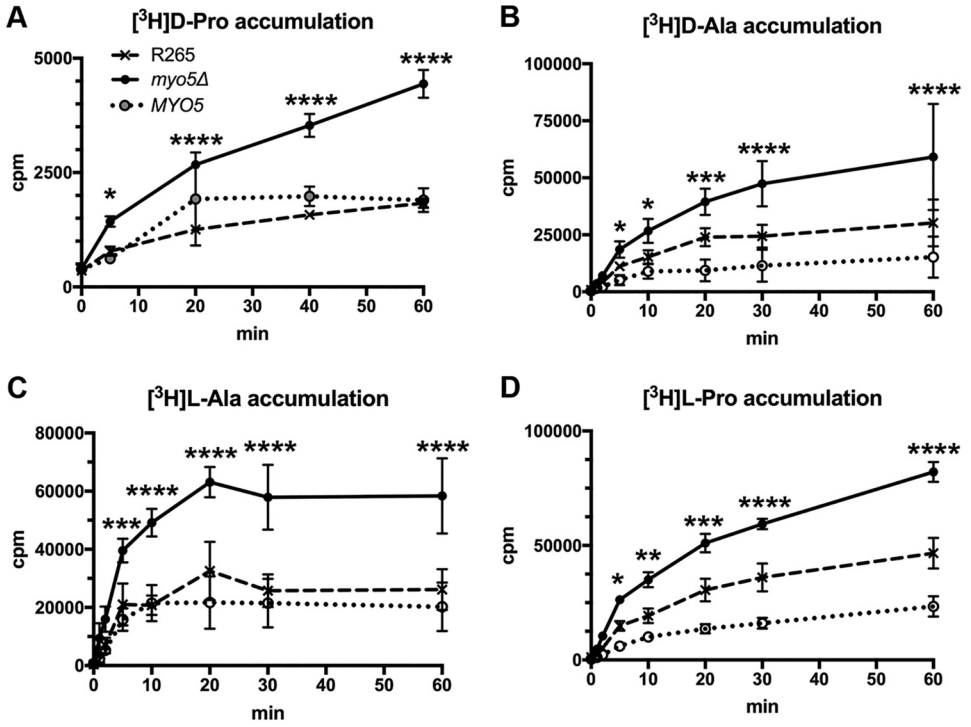

FIG 2 The *myo5*Δ mutant accumulates high levels of amino acids. Log-phase cells of the wild type, *myo5*Δ mutant, and the *myo5*Δ complemented strain (*MYO5*) were incubated with the indicated ^{3}H-labeled amino acids, and the time course of intracellular accumulation of each amino acid was determined. The experiments were repeated three times, and the error bars represent the standard deviations. Two-way ANOVA with Dunnett's multiple-comparison test was used to compare the differences at the indicated time points between the corresponding R265 strain and *myo5*Δ mutant (*, $P < 0.0332$; **, $P < 0.0021$; ***, $P < 0.0002$; ****, $P < 0.0001$).

mutant grew poorly on media supplemented with 100 mM D-proline, and its growth was slightly reduced on media supplemented with 100 mM D-alanine (Fig. 1D, top). In addition, the lowest concentration of the supplemented D-proline to cause visible growth reduction in the *myo5*Δ mutant was 5 mM (Fig. 1D, bottom). Together, these data suggested that the growth defect of the *myo5*Δ mutant may not be due to a loss of the D-amino acid utilization pathway but may instead be due to toxicity of excess D-amino acids. To test this hypothesis, we measured the accumulation of [^{3}H]D-proline and [^{3}H]D-alanine in the cells. Figure 2A and B show that the accumulation of tritium-labeled amino acids is significantly higher in the *myo5*Δ mutant than in the control strains. These results are consistent with the hypothesis that the *myo5*Δ cells accumulate D-amino acids from the culture media which causes growth retardation due to toxicity of excess D-amino acids. To our surprise, however, when we measured the uptake of [^{3}H]L-proline or L-alanine as a control, the accumulation of tritium-labeled amino acids was also significantly higher in the *myo5*Δ mutant than in the control strains (Fig. 2C and D). This observation prompted us to speculate that deletion of *MYO5* may have caused changes in membrane permeability and affected the cell's ability to take up or transport substrates from outside the cells.

To examine the possible importance of Myo5 in membrane permeability, we compared the staining patterns of three different membrane-permeant dyes. ER-Tracker Red stains the endoplasmic reticulum. CellTracker Green CMFDA is a colorless and nonfluorescent dye until its acetate groups are cleaved by intracellular esterases. MitoTracker Red CMXRos contains a mildly thiol-reactive chloromethyl moiety that labels mitochondria. The localization patterns of these dyes were according to the property of individual dyes as expected and were similar between the cells of the *myo5*Δ mutant and the wild type (Fig. 3). However, the signal intensity of each dye was considerably higher in the *myo5*Δ cells than in the wild type. These data indicate that

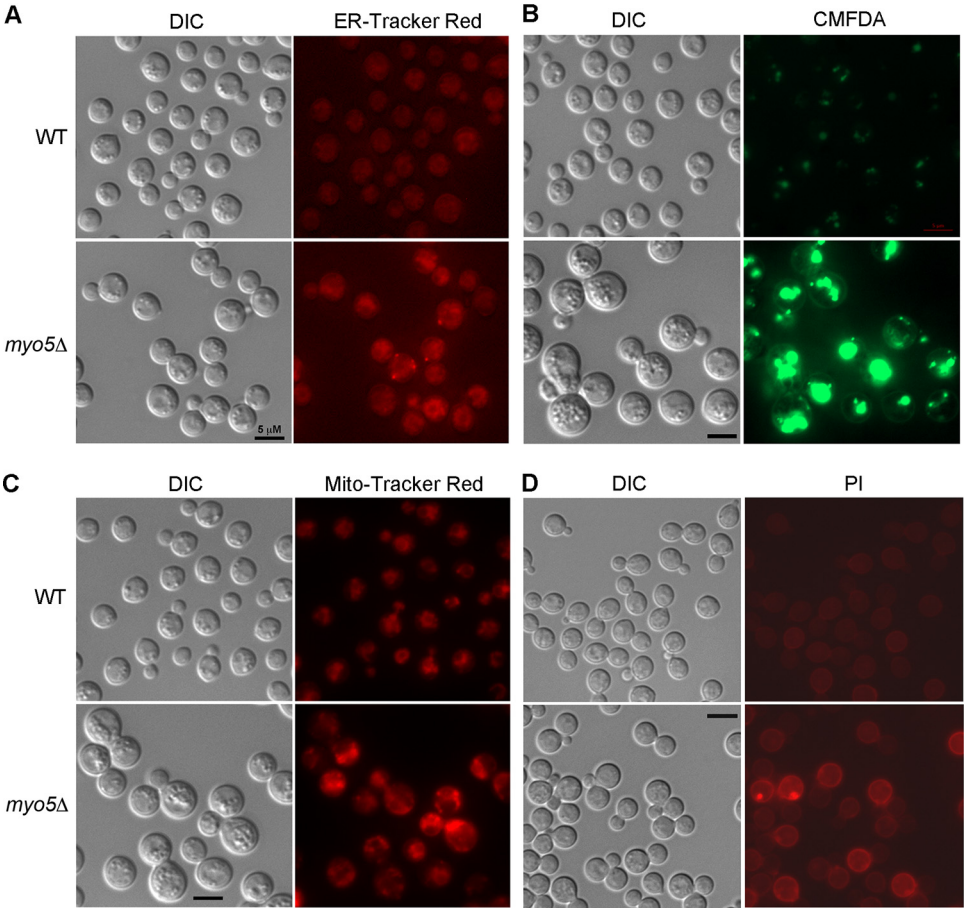

FIG 3 The *myo5*Δ mutant accumulates high levels of membrane-permeant and -nonpermeant dyes as determined by microscopy. (A to D) Cells were incubated with the indicated fluorescent dyes and observed with a microscope. (A) ER-Tracker Red. (B) CellTracker Green CMFDA. (C) MitoTracker Red CMXRos. (D) Propidium iodide (PI). Fluorescent and DIC images were photographed. The staining patterns of each dye were similar between the wild type (WT) and the *myo5*Δ mutant, but the fluorescent intensity was greater in the *myo5*Δ mutant than in the wild type. Bars = 5 μm.

deletion of *MYO5* affects neither the specificity nor distribution of the membrane-permeant dyes but allows higher accumulation of the fluorescence dyes within the cell. Quantitation of the fluorescence intensity by flow cytometry confirmed that the fluorescence intensity of all three membrane-permeant dyes was higher in the *myo5*Δ cells than in the wild type (Fig. 4A). To further characterize the importance of *MYO5* in membrane permeability, we compared the staining patterns of a membrane-nonpermeant dye, propidium iodide (PI). PI is a positively charged membrane-impermeable molecule that is generally excluded from viable cells. The PI staining patterns were similar between the *myo5*Δ mutant and the wild type, but the *myo5*Δ mutant clearly accumulated more PI than the wild type did (Fig. 3D and Fig. 4A). Together, these results support the possible alteration of the membrane permeability in the *myo5*Δ mutant.

Since the deletion of *MYO5* affected substrate accumulation, it was probable that the *myo5*Δ mutant could also accumulate larger amounts of antifungal drugs and cause hypersensitivity to the drugs. We determined the susceptibility of the *myo5*Δ mutant to several antifungal drugs by using E-tests, including flucytosine, amphotericin B, and three triazoles, fluconazole, itraconazole, and voriconazole. It was clear that the *myo5*Δ mutant had lower MICs and was hypersensitive toward all antifungal drugs compared to strain R265 (Table 1). These observations suggested that the *myo5*Δ mutant accumulates higher levels of the drugs, leading to its hypersensitivity. To validate such a

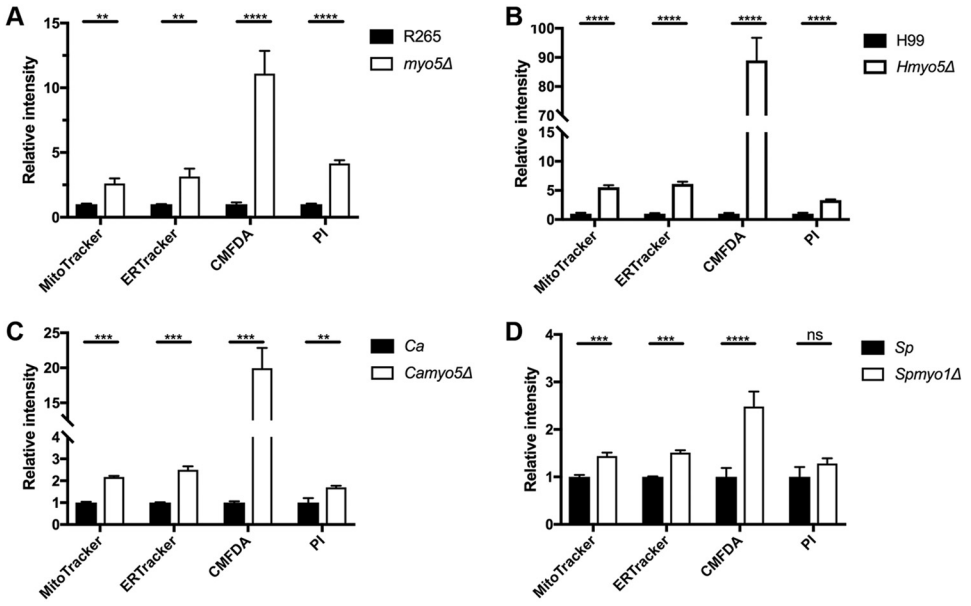

FIG 4 Myosin-I mutants of different fungal species accumulate high levels of membrane-permeant or -nonpermeant dyes. Cells of indicated strains were incubated with each membrane-permeant or -nonpermeant dye, and accumulation of each dye was assessed by flow cytometry. The experiments were repeated three times, and the error bars represent the standard deviations. *Ca*, *C. albicans*; *Sp*, *S. pombe*. Values that are significantly different are indicated by bars and asterisks as follows: **, $P \leq 0.01$; ***, $P \leq 0.001$; ****, $P \leq 0.0001$. Values that are not significantly different ($P > 0.05$) are indicated (ns).

possibility, we quantified the time course accumulation of [^{3}H]flucytosine in the wild type and the *myo5*Δ mutant. Compared to the wild type, *myo5*Δ cells accumulated substantially more [^{3}H]flucytosine (Fig. 5A), attesting that the high accumulation of flucytosine results in its hypersensitivity to flucytosine in the *myo5*Δ mutant.

Deletion of *MYO5* does not affect the distribution of permeases. It is known that amino acids and flucytosine generally enter cells through transporters/permeases. For instance, several amino acid permeases can regulate the uptake of L-amino acids in *C.*

TABLE 1 MICs of antifungal drugs

Strain or species	MIC (μg/ml)[a]				
	5-FC	AmB	Flc	Itr	Vor
R265	0.19	2	16	0.5	0.19
*myo5*Δ	0.094	0.75	3	0.19	0.047
*vrp1*Δ	0.047	1.0	8	0.38	0.094
*arp2*Δ	0.064	1.0	0.032	0.002	0.003
*arp3*Δ	0.016	0.5	0.75	0.016	0.008
C. albicans	0.094	2	1[b]	0.016[b]	0.023
*Camyo5*Δ	0.016	1.0	0.125[b]	0.008[b]	0.008
S. pombe	Resistant	0.75	32	0.094	0.25
*Spmyo1*Δ	Resistant	0.5	16	0.032	0.047
H99	0.19	2	32	1.0	0.094
*Hmyo5*Δ	0.016	0.75	16	0.5	0.047
*las17*Δ	0.032				
*sla1*Δ	0.125				
KN99	0.125				
*abp1*Δ	0.125				
*crn1*Δ	0.125				
B3501	0.047				
*abp1*Δ	0.047				
*sla2*Δ	0.047				

[a]Drug abbreviations: 5-FC, 5-fluorocytosine; AmB, amphotericin B; Flc, fluconazole; Itr, itraconazole; Vor, voriconazole.

[b]Test was done on YNB medium.

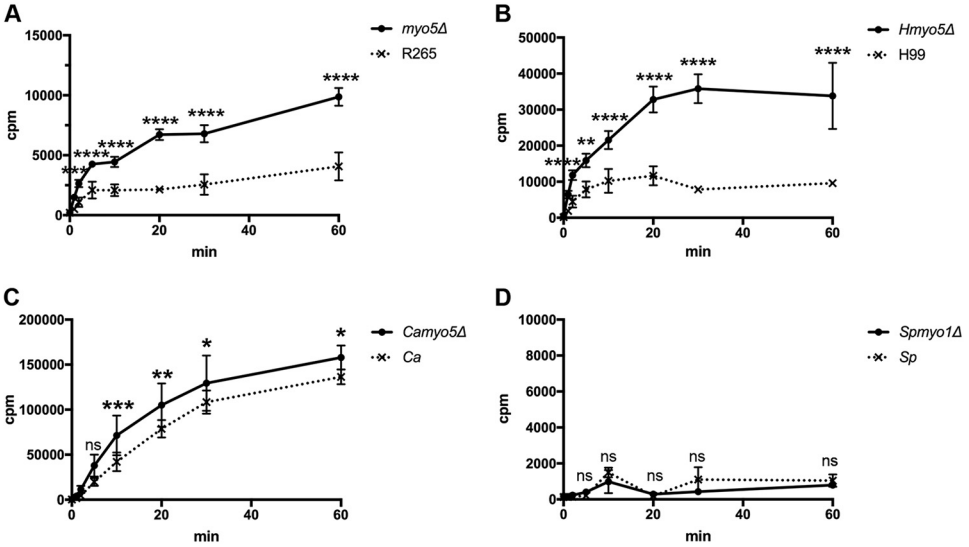

FIG 5 Myosin-I mutants of different fungal species accumulate higher levels of flucytosine. Cells of the indicated strains were incubated with [^{3}H]labeled flucytosine, and the time course of intracellular accumulation of ^{3}H was determined. The experiments were repeated three times, and the error bars represent the standard deviations. *Ca*, *C. albicans*; *Sp*, *S. pombe*. Two-way ANOVA with Dunnett's multiple-comparison test was used to compare the differences at the indicated time point between the corresponding R265 strain and the *myo5*Δ mutant (ns, not significant; *, $P < 0.0332$; **, $P < 0.0021$; ***, $P < 0.0002$; ****, $P < 0.0001$).

neoformans (30, 31), and transport of cytosine/flucytosine requires the function of transporters in *Candida* species and *S. cerevisiae* (32, 33). Since permeases are normally removed from the cell surface by endocytosis, the endocytosis defect in the *myo5*Δ mutant might result in higher levels of permeases on the cell surface, an alternative explanation for increased accumulation of substrates in the mutants. To address this possibility, we attempted to tag the permeases and studied their localization. In order to tag the appropriate permeases, we first identified the permease for flucytosine by deleting the gene encoding the putative purine-cytosine permease (CNBG_3227) in strain R265 which shares high similarity to the *S. cerevisiae* Fcy2. When the *FCY2* gene was deleted, the resulting strains were resistant to flucytosine (Fig. 6A), suggesting that the R265 *FCY2* functions as the purine-cytosine permease, as is the case in *S. cerevisiae*. To identify the permease(s) for proline, we first deleted the two putative proline permease genes (CNBG_4785 and CNAG_00597) which show high similarity to the proline permease genes identified in *C. neoformans* (30). However, deletion of both genes individually or in combination did not affect the proline utilization in R265. As an alternative approach to identify permease genes, we made use of a preliminary RNASeq data set for WM276, another genome-sequenced strain of the *C. gattii* species complex. *C. gattii* strain WM276 was grown in media containing ammonium sulfate or proline as the sole nitrogen source for the RNAseq experiment (data not shown [to be presented in a separate study]). We identified two putative amino acid transporter genes CGB_J2080C and CGB_F2450W, whose transcripts were highly induced in the cells grown in proline (67.3- and 61.6-fold increase, respectively). We then deleted the putative orthologs of these two genes in strain R265, CNBG_6051 and CNBG_1852, respectively, and found that only CNBG_1852, which we designated *AAP9*, was required for R265 to grow in D- or L-proline as the sole nitrogen source, indicating that Aap9 is the permease for D- and L-proline in R265 (Fig. 6B). We tagged Fcy2 and Aap9 with the green fluorescent protein (GFP) at its native locus, respectively, and confirmed that GFP tagging of either protein did not affect the function of the gene in flucytosine resistance and D- and L-proline utilization (data not shown). Next, we examined the localization of Fcy2 and Aap9 in strain R265 and the *myo5*Δ mutant and found that the fluorescent intensity of both proteins was indistinguishable between the *myo5*Δ mutant and R265 (Fig. 6C and D). These results indicate that a defect in *myo5*Δ does not

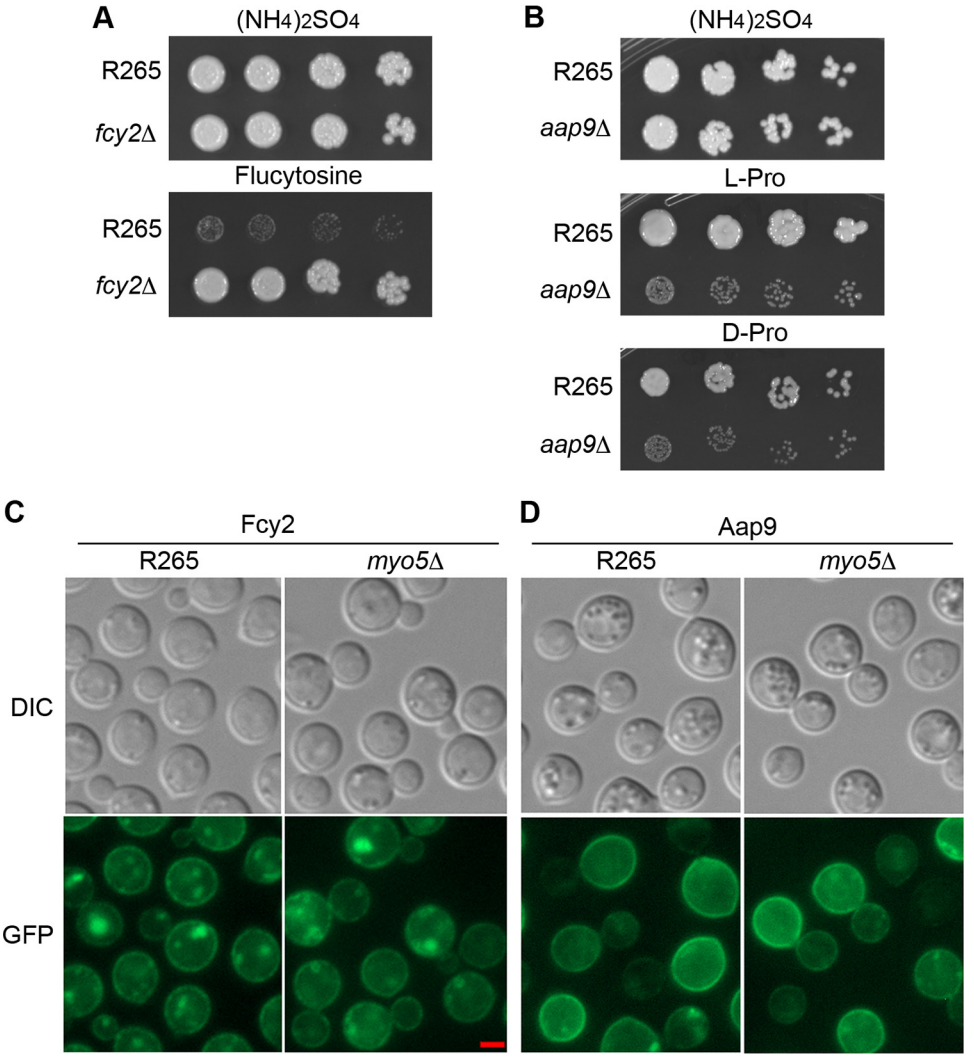

FIG 6 (A) *FCY2* is required for resistance to flucytosine. Cells of the indicated strains were spotted on YNB medium with or without 0.5 μg/ml of flucytosine. (B) *AAP9* is required for the growth in media containing D-/L-proline as the sole nitrogen source. Cells of the indicated strains were spotted on media containing 10 mM ammonium sulfate, L-proline, or D-proline. Plates were incubated at 30°C for 3 days and photographed. (C and D) Deletion of *MYO5* does not affect the distribution of transporters for flucytosine or proline. The Fcy2 and Aap9 proteins were separately tagged with green fluorescent protein in the *myo5*Δ mutant and the wild type, respectively. Strains were grown in YPD (C) or YNB supplemented with 10 mM Asn as the sole nitrogen source (D). Fluorescent and DIC images were taken from log-phase cells. Bar = 2 μm.

affect the distribution of both permeases, and as such, the observed phenotypes in the accumulation of D-/L-proline and flucytosine are not due to the endocytic defect of the *myo5*Δ mutant in removing permeases from the cell surface.

Deletion of *MYO5* affects the rate of accumulation and efflux. Since accumulation of substrates inside the cells depends on both the rate of influx as well as efflux of the substrates, we compared the efflux rates between the wild type and the *myo5*Δ mutant. Fluorescein diacetate (FDA) has been used for studying the properties of membrane permeability by measuring the kinetics of intracellular accumulation and efflux of fluorescein (34, 35). We first evaluated the time course accumulation of fluorescein in both strain R265 and the *myo5*Δ mutant. As shown in Fig. 7A, the *myo5*Δ mutant accumulates more fluorescein and faster than R265 does. After cells were loaded with a similar quantity of fluorescein, the cells were washed to remove residual FDA, and the efflux rate of fluorescein was determined. It was clear that the fluorescein efflux rate was higher in the *myo5*Δ mutant than in R265 (Fig. 7B). Thus, deletion of

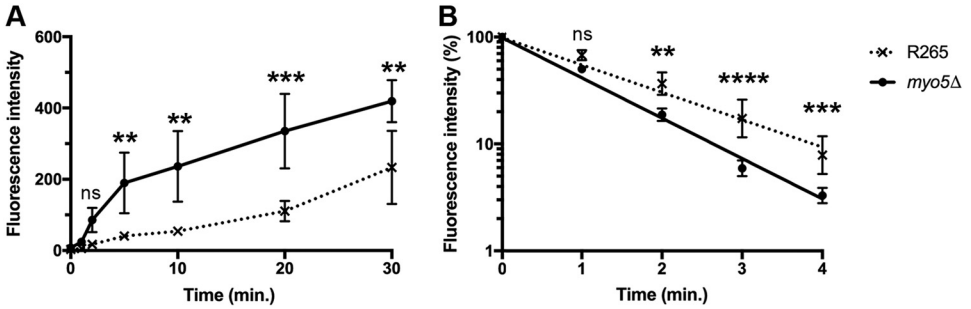

FIG 7 Fluorescein accumulation and efflux rate are higher in the *myo5*Δ mutant. (A) Time course of intracellular fluorescein accumulation. Cells were incubated with 10 μM FDA, and cellular fluorescent intensity was determined at the indicated time by flow cytometry. (B) Kinetics of fluorescein efflux. Cells were loaded with similar amounts of fluorescein, and the efflux of fluorescein was determined by measuring the intracellular fluorescent intensity by flow cytometry. The experiments were repeated three times, and the error bars represent standard deviations. Two-way ANOVA with Dunnett's multiple-comparison test was used to compare the differences at the indicated time point between the corresponding R265 strain and *myo5*Δ mutant (ns, not significant; **, $P < 0.0021$; ***, $P < 0.0002$; ****, $P < 0.0001$).

MYO5 affects both the accumulation and efflux of fluorescein, indicating that the membrane in the *myo5*Δ mutant is more permeable than the membrane in the wild type.

The sterol distribution is altered in the *myo5*Δ mutant. It is known that myosin-I can bind to membrane lipids (36), and myosin-I mutant displays an abnormal sterol distribution in the plasma membrane of fission yeast (13). It is possible that Myo5 may control membrane sterol distribution, which in turn regulates the membrane property, since it is known that the sterol contents can influence membrane fluidity and permeability (for a review, see reference 37). We used LCMS to measure the major sterol contents but found no difference in total concentration of ergosterol between the wild type and the *myo5*Δ mutant (Fig. 8A). To determine whether the distribution of sterol is different in the membrane, log-phase-grown cells of the wild type and *myo5*Δ were stained with filipin. Filipin is a naturally fluorescent sterol-binding antibiotic (38) and known to stain the areas of polarized growth as well as mating projections in *S. pombe* and the areas of mating projections in *S. cerevisiae* (39, 40). In the wild-type R265, filipin staining was primarily concentrated at the tip of the emerging bud (red arrowhead) and

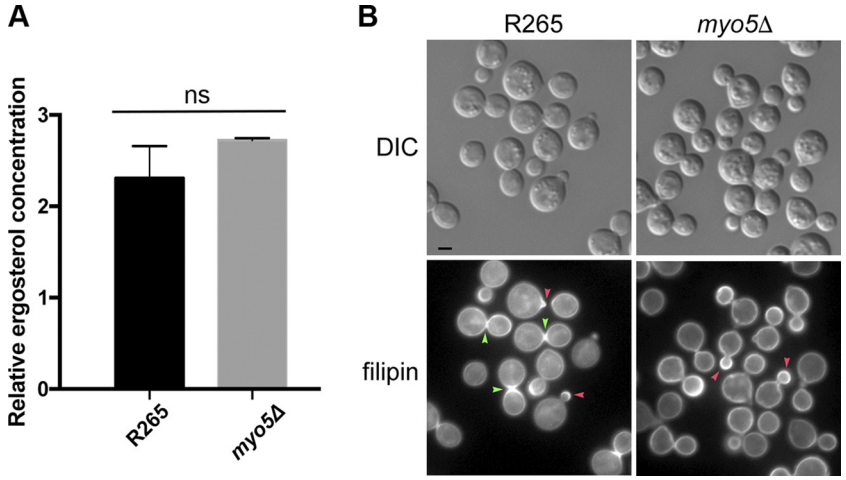

FIG 8 Ergosterol distribution appears to be altered in the *myo5*Δ mutant. (A) Ergosterol content is similar between the wild type and *myo5*Δ mutant. Ergosterol was extracted from cells and quantitated by LCMS. The experiments were repeated three times, and the error bars represent the standard deviations. (B) Filipin staining patterns are different between the wild type and the *myo5*Δ mutant. Log-phase grown cells were stained with 5 μg/ml filipin. The fluorescent and DIC images were photographed. Red arrowhead, emerging bud; green arrowhead, isthmus. Bar = 2 μm.

at the isthmus between the mother and matured daughter cells (green arrowheads) (Fig. 8B, bottom left panel), which was similar to the patterns observed in *C. neoformans* (41). We noted that the intensely stained isthmus was predominantly found in the mother-daughter pair where the size of daughter cells has reached close to 70% of the size of the mother cells (green arrowheads). This indicates that sterols were enriched at the isthmus during the later stages of cell replication before the release of daughter cells. In the *myo5*Δ mutant, filipin stained wider areas of emerging bud surface (red arrowheads) than in the wild type. In addition, intensely stained isthmus was rarely observed, and filipin staining was more evenly distributed at the cell periphery of the mother and daughter cells in the *myo5*Δ mutant. Since filipin binds sterol, it is likely that the distribution of sterol is altered in the *myo5*Δ cells and that the changes in sterol distribution are discernible in a developmental stage-dependent manner.

***MYO5* is involved in substrate accumulation in a closely related species.** To determine whether the observed *myo5*Δ phenotypes were *C. gattii* specific, we deleted *MYO5* in a closely related species, *C. neoformans* serotype A strain H99. Since *C. neoformans* cannot use D-proline as the sole nitrogen source, the D-proline growth phenotype of the H99 *myo5*Δ (H*myo5*Δ) mutant was not determined. However, as was the case with the R265 *myo5*Δ mutant, accumulation of all the membrane-permeant dyes and nonpermeant dye was markedly increased in the H*myo5*Δ mutant than in strain H99 (Fig. 4B). Similarly, the H*myo5*Δ mutant was more susceptible to all the antifungal drugs tested (Table 1) and accumulated more [^{3}H]flucytosine than the H99 strain (Fig. 5B). Therefore, *MYO5* of both *C. neoformans* and *C. gattii* plays important roles for substrate accumulation.

Myosin-I is also involved in substrate accumulation in other yeast species. It was of interest to determine whether myosin-I was involved in the substrate accumulation in other species of pathogenic and nonpathogenic yeast phylogenetically distanced from *Cryptococcus*. We found that the *myo5*Δ mutant of *C. albicans* behaves like the *myo5*Δ mutant of *Cryptococcus* species; the accumulation of all the membrane-permeant dyes and nonpermeant dye was higher in the *C. albicans myo5*Δ mutant than in the wild type (Fig. 4C), and the *C. albicans myo5*Δ mutant was hypersensitive to five antifungal drugs (Table 1). Interestingly, the levels of [^{3}H]flucytosine accumulated in the wild-type *C. albicans* was more than 10-fold higher than those in the *Cryptococcus* species, and the *C. albicans myo5*Δ mutant accumulated even more [^{3}H]flucytosine than the *C. albicans* wild type did (Fig. 5C). However, the differences in accumulation between the mutant and the wild type were smaller in *C. albicans* than in *Cryptococcus* species. The myosin-I of *S. pombe* has been designated Myo1p. We found that the *S. pombe myo1*Δ mutant accumulated more membrane-permeant dyes than the wild type did, but no significant difference was found between the wild type and *myo1*Δ in the accumulation of PI, a membrane-nonpermeant dye (Fig. 4D). Interestingly, the wild type and the *myo1*Δ mutant of *S. pombe* were intrinsically resistant to flucytosine, and both strains accumulated low levels of [^{3}H]flucytosine (Table 1 and Fig. 5D). However, the *S. pombe myo1*Δ mutant was hypersensitive to the other four antifungal drugs (Table 1). Thus, myosin-I of *C. albicans* plays a clear role in substrate accumulation, but the role of *S. pombe* myosin-I for substrate accumulation was not as versatile.

***ARP2*, *ARP3*, and *VRP1* are involved in substrate accumulation.** To determine whether other genes involved in the endocytosis process also controlled substrate accumulation, we deleted *ARP2*, *ARP3*, and *VRP1* separately in strain R265. In budding and fission yeasts, myosin-I interacts with Vrp1/WIP, which in turn binds G-actin (9, 42) and delivers actin monomers to the Arp2/3 complex (for a review, see reference 43). The genome of strain R265 contains highly conserved *ARP2* and *ARP3* and also contains a CNBG_5343 gene, which we designated *VRP1*. *VRP1* encodes a protein with a predicted WH2 motif at its N terminus and shares low similarity with Vrp1 of *S. cerevisiae*. Figure 9A shows that deletion of *ARP2* or *ARP3* in strain R265 showed a severe growth defect in D-proline and D-alanine utilization. The growth of the *vrp1*Δ mutant on D-proline and D-alanine was slightly reduced, and the growth defect was not

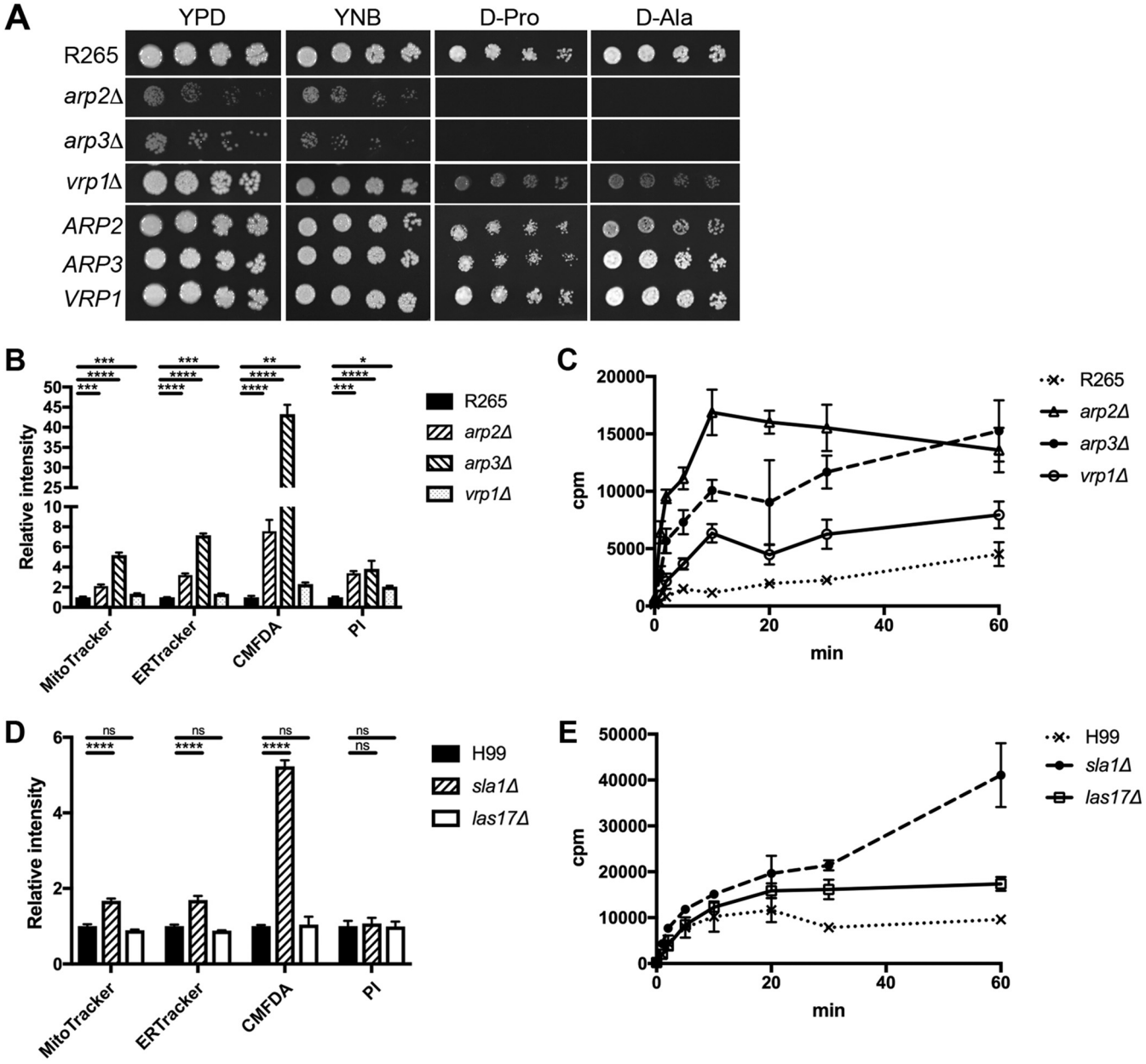

FIG 9 Several genes involved in endocytosis play a role in membrane permeability. (A) *ARP2*, *ARP3*, and *VRP1* are important for D-proline utilization. Cells of the indicated mutants and the corresponding complemented strains (*ARP2*, *ARP3*, and *VRP1*) were serially diluted and spotted on the indicated media. Plates were incubated at 30°C for 3 days and photographed. (B and C) Deletion of *ARP2*, *ARP3*, and *VRP1* causes accumulation of different fluorescent dyes (B) or [^{3}H]flucytosine (C). (D and E) Not every endocytic mutant accumulates different fluorescent dyes (D) or [^{3}H]flucytosine (E). (ns, not significant [$P > 0.05$]; *, $P \leq 0.05$; **, $P \leq 0.01$; ***, $P \leq 0.001$; ****, $P \leq 0.0001$).

as severe as in the *myo5*Δ mutant. Furthermore, complementation of each mutant with its wild-type gene restored the growth defect of each mutant (Fig. 9A). The *arp2*Δ, *arp3*Δ, and *vrp1*Δ mutants were hypersensitive toward antifungal drugs compared to the wild type (Table 1). Similarly, the accumulation of membrane-permeant dyes and nonpermeant dye was significantly higher in the *arp2*Δ, *arp3*Δ, and *vrp1*Δ mutants than in the wild type, although the amount of accumulation in the *vrp1*Δ mutant was not as dramatically increased as in the *myo5*Δ, *arp2*Δ, and *arp3*Δ mutants (Fig. 9B). In addition, the *arp2*Δ, *arp3*Δ, and *vrp1*Δ mutants accumulated higher levels of [^{3}H]flucytosine than the wild-type strain did (Fig. 9C). These results suggest that the three genes involved in actin nucleation also play a role in substrate accumulation.

Not all the endocytic mutants display the phenotype of substrate accumulation. To investigate whether other known components of endocytosis were involved in substrate accumulation, we took advantage of the large collection of deletion constructs available in the H99 background (Fungal Genetics Stock Center; provided by J. Lodge in 2007) and its derivative strain, KN99α (Fungal Genetics Stock Center; provided by H. Madhani in 2015). We examined the flucytosine sensitivity of the *abp1*Δ and *crn1*Δ mutants derived from strain KN99α as well as the *sla1*Δ and *las17*Δ mutants derived from strainH99. In addition, the *abp1*Δ and *sla2*Δ mutants were also available in the background of a *C. neoformans* serotype D strain, B-3501 (26). All the selected genes have been shown to be involved in endocytosis in other organisms (43). Out of the six tested strains, only the *las17*Δ and *sla1*Δ mutants displayed reduced resistance toward flucytosine compared to the respective wild-type strains (Table 1). We chose the *las17*Δ and *sla1*Δ mutants to determine the accumulation of fluorescent dyes and [^{3}H]flucytosine. The *sla1*Δ mutant, but not the *las17*Δ mutant, showed higher accumulation of the membrane-permeant dyes than strain H99 did (Fig. 9D). In contrast, the levels of accumulated membrane-nonpermeant dye, PI, were similar between *las17*Δ mutant, *sla1*Δ mutant, and the wild type. However, the accumulation of [^{3}H]flucytosine was higher in both the *las17*Δ and *sla1*Δ mutants than in H99 (Fig. 9E). Therefore, not all the endocytic mutants displayed the phenotype of substrate accumulation in *C. neoformans*.

DISCUSSION

Myosin-I is a molecular motor and plays various cellular roles related to membrane dynamics and trafficking. In this study, we demonstrate a hitherto unknown role of fungal myosin-I in controlling membrane permeability. We showed that the *C. gattii myo5*Δ mutant accumulates three types of molecules that can enter cells by different means: membrane-permeant molecules, membrane-nonpermeant molecules, and transporter/permease-mediated molecules. It is possible that the increased accumulation of the membrane-permeant molecules can be attributed to disrupted membrane recycling due to endocytosis defect rather than increased membrane permeability. However, microscopic examination showed no accumulation of fluorescence dyes on the cell surface, and the location of each fluorescent dye within the cells was similar for the *myo5*Δ mutant and the wild type, except for much higher fluorescent intensities in the *myo5*Δ mutant. Additionally, there was no noticeable deficiency in removing permeases/transporters from the cell surface in the *myo5*Δ mutant, indicating that the substrate accumulation phenotype was not likely due to a defect in permease recycling by endocytosis. In addition, the kinetics of fluorescein accumulation and efflux rates were higher in the *myo5*Δ mutant. These results indicate that the *myo5*Δ mutant in *C. gattii* has altered membrane permeability. Furthermore, we show that involvement of myosin-I in substrate accumulation is common among four different fungal species tested, although it was less clear in *S. pombe*. Together, these data indicate that fungal myosin-I plays a role in controlling membrane permeability, which has not been reported in other eukaryotic organisms.

The importance of myosin-1 for endocytosis has been well established. There are more than 50 different proteins involved in endocytosis (43–45) which form functional modules in different stages of endocytosis and are recruited to the endocytic site with an organized spatial and temporal order (44, 46, 47). In the current study, we have selected many genes known to be associated with the process of endocytosis in other organisms, including the genes involved in the formation stages of the coat complex (*sla1*Δ and *sla2*Δ), WASP/Myo module (*las17*Δ, *vrp1*Δ, and *myo5*Δ), and actin network (*arp2*Δ, *arp3*Δ, *abp1*Δ, and *crn1*Δ). Interestingly, mutants from each stage of endocytosis either displayed or did not display the substrate accumulation phenotype, and the levels of accumulated substrates were not the same among all those that displayed the phenotype. Thus, our results not only indicate that several genes functioning in endocytosis play a role in controlling substrate accumulation, but also exhibit the complexity of the relationship between membrane permeability and endocytosis. It is

not clear whether severities of endocytic defects vary among these mutants or what the nature of the relationship between endocytosis and substrate accumulation phenotype is. Future studies in quantification of endocytic defects and the extent of miscellaneous substance accumulation in different endocytic mutants may provide insights into their biological connections with altered membrane permeability.

How does a type I fungal myosin, a molecular motor, control substrate accumulation? It is possible that the putative motor function and/or lipid interacting function of type I myosin together with the components involved in endocytosis process may modulate the functions of transporters and regulate the properties of membrane permeability. It has been shown that type I myosin can bind to membrane lipids (36). Furthermore, the *S. pombe* myosin-I, myo1p, is required for proper organization of the large sterol-rich membrane domains (13). It has been proposed that the basic TH1 domain of myo1p may bind to phospholipids that directly affect the local composition of the membrane, or alternatively, myo1p may contribute to membrane tension and could affect membrane organization (48). Since it is known that sterols can influence membrane fluidity and permeability (for a review, see reference 37), it is probable that the changes in sterol organization have contributed to the observed alterations in membrane characteristics. By filipin staining, we showed that deletion of *MYO5* perturbs organization of the large sterol-rich domains. Filipin is a traditional sterol marker (38), and it has been used to stain the large sterol-rich domains in several fungal species (41, 49). The likelihood of altered sterol organization in the myosin-I mutants was further supported by their hypersensitivity to amphotericin B (Table 1). Amphotericin B is known to target ergosterol to form aggregates and increase the permeability of the cell membrane (50, 51) or to extract ergosterol from lipid bilayers and kill fungal cells (52). However, the detailed mechanisms of interaction between myosin-I and sterol/lipids for the regulation of membrane properties remain to be elucidated. It is also currently unknown whether the contents or distribution of membrane lipids have been modified in the *myo5*Δ mutant. Future studies focused on lipidomics may shed light on the possible relationship between type I myosin and the structures, functions, and dynamics of cellular lipids. Finally, since myosin-I mutants were hypersensitive to several antifungal drugs and the carboxyl-terminal tail of fungal myosin-I is different from the tail of human myosin-I (see Fig. S1 in the supplemental material), it is possible that combination therapy with drugs targeting the fungal myosin or components of endocytosis process may offer new treatments for fungal infections.

MATERIALS AND METHODS

Strains and culture conditions. Strains relevant to the study are listed in Table S1 in the supplemental material. Standard culture conditions and microbiological methods were used as described previously (23). Spot assays were performed on yeast extract-peptone-dextrose (YEPD) or yeast nitrogen base (YNB) without amino acids and without ammonium sulfate (YNB-A-N; 1.7g/liter) with 2% glucose supplemented with 10 mM indicated nitrogen sources.

Gene manipulation. The entire protein coding sequence of genes of interest were deleted by homologous recombination as described previously (23). Homologous integration was confirmed by PCR and Southern blot analysis (data not shown). Deletants were complemented by homologous integration using biolistic transformation. The *MYO5*, *FCY2,* and *AAP9* genes were tagged with mNG (24) at its native locus to visualize its localization.

Microscopy. A Zeiss Axiovert fluorescence microscope equipped with an AxioCam MRm digital camera was used to take differential interference contrast (DIC) microscopy and fluorescent images. The exposure times and other microscope settings were held constant between compared images. An endocytosis assay of FM4-64 and Lucifer yellow was performed as described previously (53). Filipin staining was carried out as described previously (54) at a final concentration of 5 μg/ml for 2 min at room temperature.

Amino acids and flucytosine accumulation assay. For amino acid uptake assays, cells were grown to log phase in YNB medium containing 10 mM asparagine as the sole nitrogen source. Cells were harvested, washed with cold YNB-A-N without glucose, and adjusted to 10 optical density units/ml. Each 100 μl of cells was mixed with 100 μl of YNB-A-N with glucose supplemented with 0.5 mM concentration of assayed amino acid and 0.5 μCi of ^{3}H-labeled assayed amino acid. The ^{3}H-labeled amino acid used in the experiment was D-[3,4-^{3}H]proline (40 Ci/mmol; 1 mCi/ml) (Moravek Inc.), L-[3,4-^{3}H]proline (60 Ci/mmol; 1 mCi/ml) (Moravek Inc.), D-[2,3-^{3}H]-alanine (60 Ci/mmol; 1 mCi/ml) (Moravek Inc.), and L-[2,3-^{3}H]alanine (55 Ci/mmol; 1 mCi/ml) (Moravek Inc.). Cells were incubated at 30°C in a water bath shaker, and 50-μl aliquots of the sample were removed at 0, 1, 2, 5, 10, 20, 30, and 60 min and added to 2 ml

ice-cold YNB-A-N supplemented with 50 mM concentration of the assayed amino acid. Cells were immediately filtered with 24-mm Whatman GF/C filter and washed with cold YNB-A-N and assayed for radioactivity. The flucytosine accumulation assay was performed as described previously with modifications (55). The cells were grown and harvested as described above. Each 100 μl of cells was mixed with 100 μl of 2× Asn media with glucose supplemented with 200 μM flucytosine and 0.8 μCi of [^{3}H]flucytosine (4.0 Ci/mmol; 1 mCi/ml) (Moravek Inc.). Cells were incubated at 30°C in a water bath shaker, and 50-μl aliquots of sample were removed at 0, 1, 2, 5, 10, 20, 30, and 60 min and added to 2 ml of cold media containing 20 mM flucytosine. Cells were immediately filtered with 24-mm Whatman GF/C filter, washed with cold YNB-A-N, and assayed for radioactivity.

Uptake of fluorescent dyes. Each strain was grown to the log phase in 10 mM Asn media and adjusted to an optical density at 600 nm (OD_{600}) of 0.3. Cells were incubated at 30°C for 30 min in the presence of 0.1 μM Mito Tracker Red CMXRos, 5 μM CMFDA, or 1 μM ER-Tracker Red. For propidium iodide staining, cells were washed with phosphate-buffered saline (PBS) and treated with 10 μg/ml of dye for 10 min at room temperature (RT). The accumulation of each dye was immediately assessed by flow cytometry or by observation with a microscope. For each sample, 30,000 events were analyzed using Flow Jo software. FDA accumulation and efflux rate measurement were performed as described previously with modifications (34). For FDA accumulation, log-phase-grown cells were washed in ice-cold 10 mM potassium phosphate (pH 6.0) and adjusted to an OD_{600} of 0.8. FDA was added to 10 μM and incubated at 30°C. At the indicated time, 100 μl of cells was taken out and transferred to 400 μl of ice-cold 10 mM potassium phosphate (pH 6.0) and analyzed immediately by flow cytometry. For fluorescein efflux, a similar amount of fluorescein was loaded to each strain by controlling the time of incubation with FDA as described above. The cells were washed in ice-cold 10 mM potassium phosphate (pH 6.0) and resuspended in 1 ml of ice-cold potassium phosphate (pH 6.0). Cells were removed from ice and incubated at room temperature. At the indicated time, 100 μl of cells was taken out and transferred to 400 μl of ice-cold 10 mM potassium phosphate (pH 6.0) and analyzed immediately by flow cytometry. Efflux rate constants were calculated from the slopes of the fitted lines obtained by regression analysis.

Drug susceptibility test. MICs of different drugs, flucytosine (5-FC), amphotericin B (AmB), fluconazole (Flc), itraconazole (Itr), and voriconazole (Vor), were determined by plating 2×10^6 cells on YEPD or YNB agar plates followed by application of Epsilometer test strips (Etest strips; AB Biodisk). The plates were incubated at 30°C, and photographs were taken after 72 h.

Sterol analysis. Log-phase-grown cells were used for sterol extraction as described previously with modification (56). The extracted sterols were analyzed and characterized by liquid chromatography/mass spectrometry (LCMS). LCMS analysis was performed with a Waters Acquity I-class UPLC (Waters Corp., Milford, MA) and a Thermo Scientific Q-Exactive mass spectrometer (high resolution – accurate mass) with a HESI-II electrospray source in positive ion mode and at a resolution of 35,000. Samples were kept at 5°C in the temperature-controlled autosampler. The separation was performed with a sample volume injection of 1 μl on a 1.6-μm Cortecs C_8 column (2.1 by 100 mm) (Waters Corp., Milford, MA) maintained at 40°C. Each sample was analyzed three times with separate injections. The isocratic chromatography used solvent A (2% H_2O with 0.1% formic acid) and solvent B (98% methanol [MeOH] with 0.1% formic acid) at a flow rate of 250 μl/min. The mass spectrometer method used a full scan function from *m/z* 300 to 450 without a lock mass. The compounds were identified by a comparison with the standards (cholesterol, ergosterol, and lanosterol) on the basis of their retention time and high-resolution accurate-mass (HR-AM) mass spectrometry, or tentatively identified (squalene, ergosta-7-enol, eburicol, 4-alpha-methylfecosterol) by HR-AM mass spectrometry.

Statistical analysis. All experiments were performed in triplicate, and statistics and graphs were obtained using Graph Pad Prism 7. Student's *t* test and analysis of variance (ANOVA) followed by multiple-comparison test were used to determine whether there are significant differences between the indicated samples.

SUPPLEMENTAL MATERIAL

Supplemental material for this article may be found at https://doi.org/10.1128/mBio.01867-19.

FIG S1, PDF file, 0.1 MB.

TABLE S1, DOCX file, 0.01 MB.

ACKNOWLEDGMENTS

We thank P. J. Espenshade and M. Whiteway for providing the *S. pombe* and *C. albicans* strains, respectively. Deletion strains of KN99 and H99 were obtained from the Fungal Genetics Stock Center (Manhattan, Kansas, USA). We also thank Shannon Moyer and Michael Davis for critical reading of the manuscript.

This work was supported by the Division of Intramural Research (DIR), NIAID, NIH.

REFERENCES

1. Sellers JR. 2000. Myosins: a diverse superfamily. Biochim Biophys Acta 1496:3–22. https://doi.org/10.1016/s0167-4889(00)00005-7.
2. Coluccio LM. 2008. Myosin I, p 95–124. *In* Coluccio LM (ed), Myosins: a superfamily of molecular motors. Springer, Dordrecht, The Netherlands. https://doi.org/10.1007/978-1-4020-6519-4.
3. Masters TA, Kendrick-Jones J, Buss F. 2017. Myosins: domain organisa-

tion, motor properties, physiological roles and cellular functions. Handb Exp Pharmacol 235:77–122. https://doi.org/10.1007/164_2016_29.
4. McIntosh BB, Ostap EM. 2016. Myosin-I molecular motors at a glance. J Cell Sci 129:2689–2695. https://doi.org/10.1242/jcs.186403.
5. Kim SV, Flavell RA. 2008. Myosin I: from yeast to human. Cell Mol Life Sci 65:2128–2137. https://doi.org/10.1007/s00018-008-7435-5.
6. Mermall V, Post PL, Mooseker MS. 1998. Unconventional myosins in cell movement, membrane traffic, and signal transduction. Science 279:527–533. https://doi.org/10.1126/science.279.5350.527.
7. Giblin J, Fernandez-Golbano IM, Idrissi FZ, Geli MI. 2011. Function and regulation of *Saccharomyces cerevisiae* myosins-I in endocytic budding. Biochem Soc Trans 39:1185–1190. https://doi.org/10.1042/BST0391185.
8. Goodson HV, Anderson BL, Warrick HM, Pon LA, Spudich JA. 1996. Synthetic lethality screen identifies a novel yeast myosin I gene (*MYO5*): myosin I proteins are required for polarization of the actin cytoskeleton. J Cell Biol 133:1277–1291. https://doi.org/10.1083/jcb.133.6.1277.
9. Sun Y, Martin AC, Drubin DG. 2006. Endocytic internalization in budding yeast requires coordinated actin nucleation and myosin motor activity. Dev Cell 11:33–46. https://doi.org/10.1016/j.devcel.2006.05.008.
10. Lewellyn EB, Pedersen RT, Hong J, Lu R, Morrison HM, Drubin DG. 2015. An engineered minimal WASP-myosin fusion protein reveals essential functions for endocytosis. Dev Cell 35:281–294. https://doi.org/10.1016/j.devcel.2015.10.007.
11. Kachurina N, Turcotte B, Whiteway M. 2012. Motor protein Myo5p is required to maintain the regulatory circuit controlling *WOR1* expression in *Candida albicans*. Eukaryot Cell 11:626–637. https://doi.org/10.1128/EC.00021-12.
12. Oberholzer U, Iouk TL, Thomas DY, Whiteway M. 2004. Functional characterization of myosin I tail regions in *Candida albicans*. Eukaryot Cell 3:1272–1286. https://doi.org/10.1128/EC.3.5.1272-1286.2004.
13. Takeda T, Chang F. 2005. Role of fission yeast myosin I in organization of sterol-rich membrane domains. Curr Biol 15:1331–1336. https://doi.org/10.1016/j.cub.2005.07.009.
14. Toya M, Motegi F, Nakano K, Mabuchi I, Yamamoto M. 2001. Identification and functional analysis of the gene for type I myosin in fission yeast. Genes Cells 6:187–199. https://doi.org/10.1046/j.1365-2443.2001.00414.x.
15. Kwon-Chung KJ, Bennett JE. 1992. Cryptococcosis. *In* Medical mycology. Lea & Febiger, Philadelphia, PA.
16. Ngamskulrungroj P, Chang Y, Roh J, Kwon-Chung KJ. 2012. Differences in nitrogen metabolism between *Cryptococcus neoformans* and *C. gattii*, the two etiologic agents of cryptococcosis. PLoS One 7:e34258. https://doi.org/10.1371/journal.pone.0034258.
17. Dufait R, Velho R, De Vroey C. 1987. Rapid identification of the two varieties of *Cryptococcus neoformans* by D-proline assimilation. Mykosen 30:483.
18. Hashimoto A, Nishikawa T, Oka T, Takahashi K, Hayashi T. 1992. Determination of free amino acid enantiomers in rat brain and serum by high-performance liquid chromatography after derivatization with N-tert.-butyloxycarbonyl-L-cysteine and o-phthaldialdehyde. J Chromatogr B 582:41–48. https://doi.org/10.1016/0378-4347(92)80300-f.
19. Schell MJ, Molliver ME, Snyder SH. 1995. D-Serine, an endogenous synaptic modulator: localization to astrocytes and glutamate-stimulated release. Proc Natl Acad Sci U S A 92:3948–3952. https://doi.org/10.1073/pnas.92.9.3948.
20. D'Aniello A, D'Onofrio G, Pischetola M, D'Aniello G, Vetere A, Petrucelli L, Fisher GH. 1993. Biological role of D-amino acid oxidase and D-aspartate oxidase. Effects of D-amino acids. J Biol Chem 268:26941–26949.
21. Robinson T. 1976. D-Amino acids in higher plants. Life Sci 19:1097–1102. https://doi.org/10.1016/0024-3205(76)90244-7.
22. Friedman M. 1999. Chemistry, nutrition, and microbiology of D-amino acids. J Agric Food Chem 47:3457–3479. https://doi.org/10.1021/jf990080u.
23. Chang YC, Khanal Lamichhane A, Bradley J, Rodgers L, Ngamskulrungroj P, Kwon-Chung KJ. 2015. Differences between *Cryptococcus neoformans* and *Cryptococcus gattii* in the molecular mechanisms governing utilization of D-amino acids as the sole nitrogen source. PLoS One 10:e0131865. https://doi.org/10.1371/journal.pone.0131865.
24. Shaner NC, Lambert GG, Chammas A, Ni Y, Cranfill PJ, Baird MA, Sell BR, Allen JR, Day RN, Israelsson M, Davidson MW, Wang J. 2013. A bright monomeric green fluorescent protein derived from *Branchiostoma lanceolatum*. Nat Methods 10:407–409. https://doi.org/10.1038/nmeth.2413.
25. Riedl J, Crevenna AH, Kessenbrock K, Yu JH, Neukirchen D, Bista M, Bradke F, Jenne D, Holak TA, Werb Z, Sixt M, Wedlich-Soldner R. 2008. Lifeact: a versatile marker to visualize F-actin. Nat Methods 5:605–607. https://doi.org/10.1038/nmeth.1220.
26. Chang YC, Lamichhane AK, Kwon-Chung KJ. 2012. Role of actin-bundling protein SacVI in growth of *Cryptococcus neoformans* at low oxygen concentration. Eukaryot Cell 11:943–951. https://doi.org/10.1128/EC.00120-12.
27. Soutourina J, Plateau P, Blanquet S. 2000. Metabolism of D-aminoacyl-tRNAs in *Escherichia coli* and *Saccharomyces cerevisiae* cells. J Biol Chem 275:32535–32542. https://doi.org/10.1074/jbc.M005166200.
28. Ohnishi E, Macleod H, Horowitz NH. 1962. Mutants of *Neurospora* deficient in D-amino acid oxidase. J Biol Chem 237:138–142.
29. Champney WS, Jensen RA. 1970. Molecular events in the growth inhibition of *Bacillus subtilis* by D-tyrosine. J Bacteriol 104:107–116.
30. Martho KF, de Melo AT, Takahashi JP, Guerra JM, Santos DC, Purisco SU, Melhem MS, Fazioli RD, Phanord C, Sartorelli P, Vallim MA, Pascon RC. 2016. Amino acid permeases and virulence in *Cryptococcus neoformans*. PLoS One 11:e0163919. https://doi.org/10.1371/journal.pone.0163919.
31. Saier MH, Jr. 2000. Families of transmembrane transporters selective for amino acids and their derivatives. Microbiology 146:1775–1795. https://doi.org/10.1099/00221287-146-8-1775.
32. Fasoli MO, Kerridge D. 1990. Uptake of pyrimidines and their derivatives into *Candida glabrata* and *Candida albicans*. J Gen Microbiol 136:1475–1481. https://doi.org/10.1099/00221287-136-8-1475.
33. Weber E, Rodriguez C, Chevallier MR, Jund R. 1990. The purine-cytosine permease gene of *Saccharomyces cerevisiae*: primary structure and deduced protein sequence of the FCY2 gene product. Mol Microbiol 4:585–596. https://doi.org/10.1111/j.1365-2958.1990.tb00627.x.
34. Prosperi E, Croce AC, Bottiroli G, Supino R. 1986. Flow cytometric analysis of membrane permeability properties influencing intracellular accumulation and efflux of fluorescein. Cytometry 7:70–75. https://doi.org/10.1002/cyto.990070110.
35. Sengbusch GV, Couwenbergs C, Kuhner J, Muller U. 1976. Fluorogenic substrate turnover in single living cells. Histochem J 8:341–350. https://doi.org/10.1007/BF01003822.
36. Adams RJ, Pollard TD. 1989. Binding of myosin I to membrane lipids. Nature 340:565–568. https://doi.org/10.1038/340565a0.
37. Dufourc EJ. 2008. Sterols and membrane dynamics. J Chem Biol 1:63–77. https://doi.org/10.1007/s12154-008-0010-6.
38. Drabikowski W, Lagwińska E, Sarzala MG. 1973. Filipin as a fluorescent probe for the location of cholesterol in the membranes of fragmented sarcoplasmic reticulum. Biochim Biophys Acta 291:61–70. https://doi.org/10.1016/0005-2736(73)90060-6.
39. Wachtler V, Rajagopalan S, Balasubramanian MK. 2003. Sterol-rich plasma membrane domains in the fission yeast *Schizosaccharomyces pombe*. J Cell Sci 116:867–874. https://doi.org/10.1242/jcs.00299.
40. Bagnat M, Simons K. 2002. Cell surface polarization during yeast mating. Proc Natl Acad Sci U S A 99:14183–14188. https://doi.org/10.1073/pnas.172517799.
41. Nichols CB, Fraser JA, Heitman J. 2004. PAK kinases Ste20 and Pak1 govern cell polarity at different stages of mating in *Cryptococcus neoformans*. Mol Biol Cell 15:4476–4489. https://doi.org/10.1091/mbc.e04-05-0370.
42. Sirotkin V, Beltzner CC, Marchand JB, Pollard TD. 2005. Interactions of WASp, myosin-I, and verprolin with Arp2/3 complex during actin patch assembly in fission yeast. J Cell Biol 170:637–648. https://doi.org/10.1083/jcb.200502053.
43. Goode BL, Eskin JA, Wendland B. 2015. Actin and endocytosis in budding yeast. Genetics 199:315–358. https://doi.org/10.1534/genetics.112.145540.
44. Weinberg J, Drubin DG. 2012. Clathrin-mediated endocytosis in budding yeast. Trends Cell Biol 22:1–13. https://doi.org/10.1016/j.tcb.2011.09.001.
45. Kaksonen M, Roux A. 2018. Mechanisms of clathrin-mediated endocytosis. Nat Rev Mol Cell Biol 19:313–326. https://doi.org/10.1038/nrm.2017.132.
46. Mund M, van der Beek JA, Deschamps J, Dmitrieff S, Hoess P, Monster JL, Picco A, Nedelec F, Kaksonen M, Ries J. 2018. Systematic nanoscale analysis of endocytosis links efficient vesicle formation to patterned actin nucleation. Cell 174:884–896.e17. https://doi.org/10.1016/j.cell.2018.06.032.
47. Kukulski W, Schorb M, Kaksonen M, Briggs JA. 2012. Plasma membrane reshaping during endocytosis is revealed by time-resolved electron tomography. Cell 150:508–520. https://doi.org/10.1016/j.cell.2012.05.046.
48. Dai J, Ting-Beall HP, Hochmuth RM, Sheetz MP, Titus MA. 1999. Myosin

l contributes to the generation of resting cortical tension. Biophys J 77:1168–1176. https://doi.org/10.1016/s0006-3495(99)76968-7.
49. Alvarez FJ, Douglas LM, Konopka JB. 2007. Sterol-rich plasma membrane domains in fungi. Eukaryot Cell 6:755–763. https://doi.org/10.1128/EC.00008-07.
50. Bolard J. 1986. How do the polyene macrolide antibiotics affect the cellular membrane properties? Biochim Biophys Acta 864:257–304. https://doi.org/10.1016/0304-4157(86)90002-x.
51. Baginski M, Czub J. 2009. Amphotericin B and its new derivatives - mode of action. Curr Drug Metab 10:459–469. https://doi.org/10.2174/138920009788898019.
52. Anderson TM, Clay MC, Cioffi AG, Diaz KA, Hisao GS, Tuttle MD, Nieuwkoop AJ, Comellas G, Maryum N, Wang S, Uno BE, Wildeman EL, Gonen T, Rienstra CM, Burke MD. 2014. Amphotericin forms an extramembranous and fungicidal sterol sponge. Nat Chem Biol 10:400–406. https://doi.org/10.1038/nchembio.1496.
53. Baggett JJ, Shaw JD, Sciambi CJ, Watson HA, Wendland B. 2003. Fluorescent labeling of yeast. Curr Protoc Cell Biol Chapter 4:Unit 4.13. https://doi.org/10.1002/0471143030.cb0413s20.
54. Takeda T, Kawate T, Chang F. 2004. Organization of a sterol-rich membrane domain by cdc15p during cytokinesis in fission yeast. Nat Cell Biol 6:1142–1144. https://doi.org/10.1038/ncb1189.
55. Costa C, Ponte A, Pais P, Santos R, Cavalheiro M, Yaguchi T, Chibana H, Teixeira MC. 2015. New mechanisms of flucytosine resistance in *C. glabrata* unveiled by a chemogenomics analysis in *S. cerevisiae*. PLoS One 10:e0135110. https://doi.org/10.1371/journal.pone.0135110.
56. Chang YC, Khanal Lamichhane A, Garraffo HM, Walter PJ, Leerkes M, Kwon-Chung KJ. 2014. Molecular mechanisms of hypoxic responses via unique roles of Ras1, Cdc24 and Ptp3 in a human fungal pathogen *Cryptococcus neoformans*. PLoS Genet 10:e1004292. https://doi.org/10.1371/journal.pgen.1004292.